

Supporting information

Developing chiral aggregates exhibiting anti-S-shaped CD-*ee* dependence: Using *meso*-isomer to tune dynamic aggregates induced by enantiomers

Xiao-Yan Lin,[†] Jin-Ling Shi,[†] Qian Wang, Yue-Bo Yu, Xuan-Xuan Chen, Xiaosheng Yan, Xin Wu, Jian-Bin Lin, Zhao Li, and Yun-Bao Jiang*

Department of Chemistry, College of Chemistry and Chemical Engineering and the MOE Key Laboratory of Spectrochemical Analysis and Instrumentation, Xiamen University, Xiamen 361005, China

[†] Xiao-Yan Lin and Jin-Ling Shi contributed equally to this work.

* E-mail: ybjiang@xmu.edu.cn.

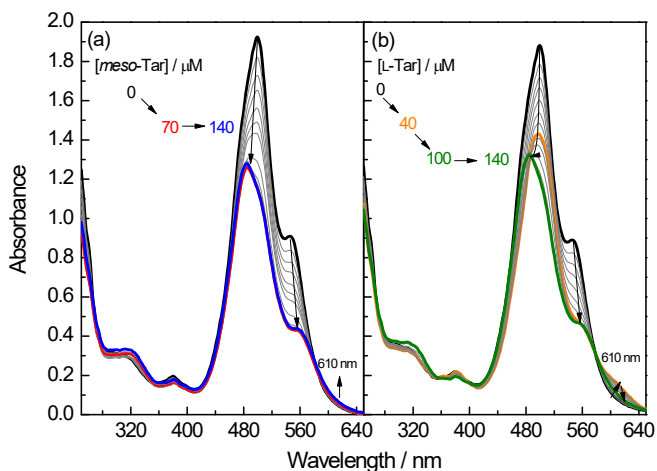


Figure S1. Absorption spectra of **1** in the presence of increasing concentration of (a) *meso*-Tar and (b) L-Tar in pH 5.0 acetate buffer containing 2.5% by volume DMSO. $[1] = 50 \mu\text{M}$.

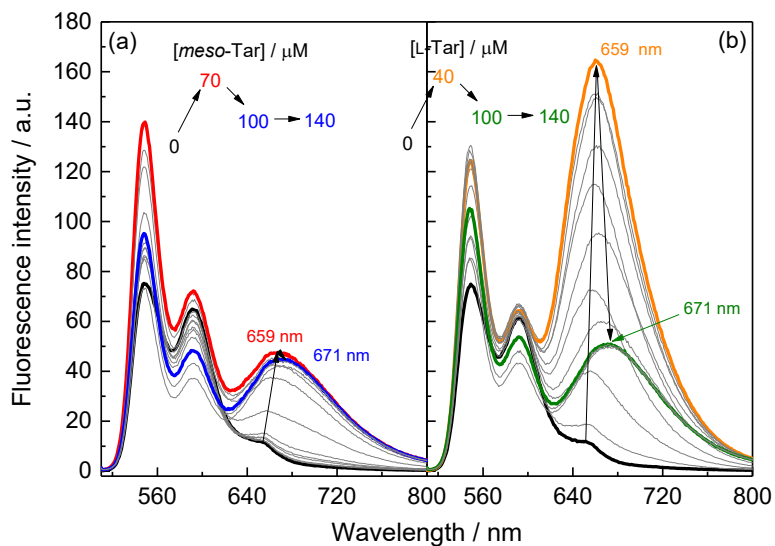


Figure S2. Fluorescence spectra of **1** in the presence of (a) *meso*-Tar and (b) L-Tar in pH 5.0 acetate buffer containing 2.5% by volume DMSO. The long-wavelength emission is due to the excimer of **1**. $[1] = 50 \mu\text{M}$; $\lambda_{\text{ex}} = 499 \text{ nm}$, $\text{slit}_{\text{ex}} = \text{slit}_{\text{em}} = 5 \text{ nm}$.

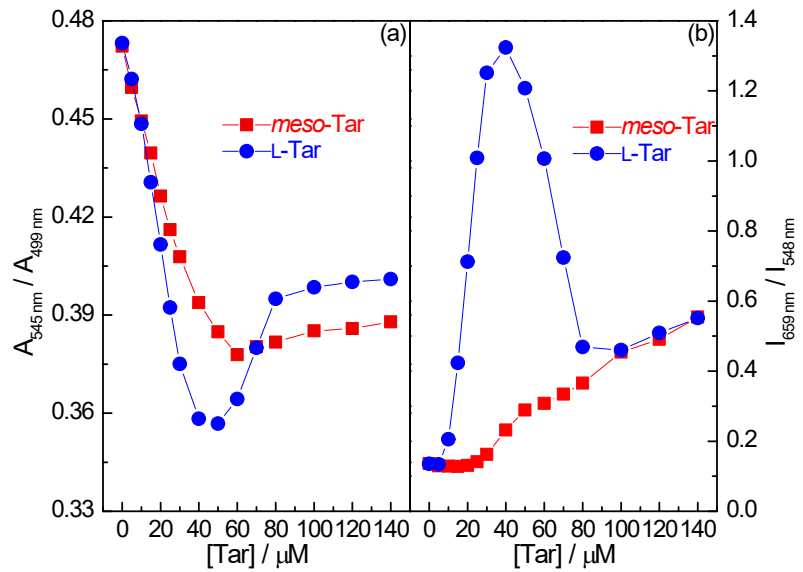


Figure S3. Ratio of (a) absorbance $A_{545\text{ nm}} / A_{499\text{ nm}}$ and (b) fluorescence intensity $I_{659\text{ nm}} / I_{548\text{ nm}}$ of **1** as a function of concentration of *meso*-Tar and *L*-Tar in pH 5.0 acetate buffer containing 2.5% by volume DMSO. $\lambda_{\text{ex}} = 499\text{ nm}$, $\text{slit}_{\text{ex}} = \text{slit}_{\text{em}} = 5\text{ nm}$.

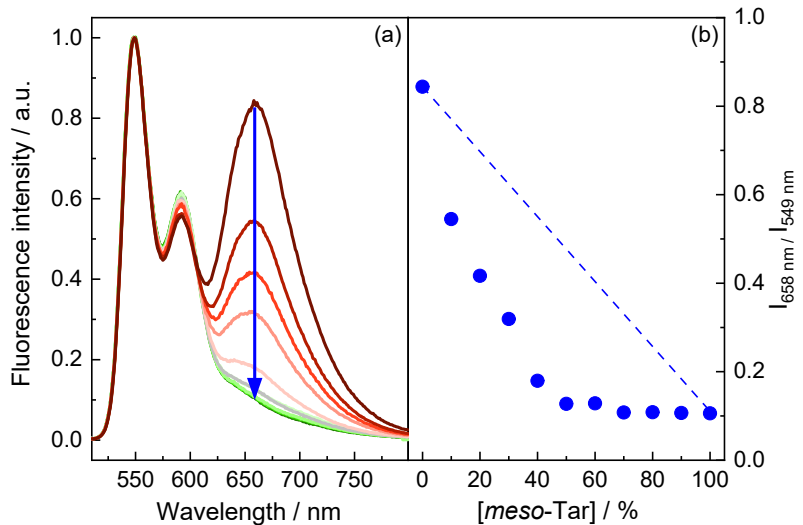


Figure S4. (a) Fluorescence spectra of **1** in the presence of *meso*- and *L*-Tar mixture of increasing molar fraction of *meso*-Tar and (b) plots of the ratio of fluorescence intensity at 658 nm to that at 549 nm versus molar fraction of *meso*-Tar in pH 5.0 acetate buffer containing 2.5% by volume DMSO. Emission at long-wavelength of 659 nm is due to the excimer of **1**. $[1] = 50\text{ }\mu\text{M}$, $[\text{L-Tar}] + [\text{meso-Tar}] = 30\text{ }\mu\text{M}$.

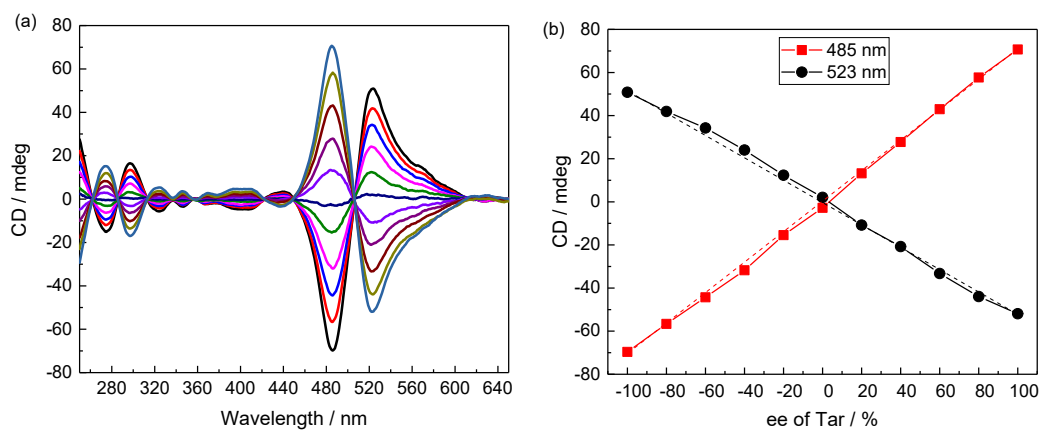


Figure S5. (a) CD spectra of **1** in the presence of Tar of different *ee* and (b) CD-*ee* dependence of the **1**-Tar assembly in pH 5.0 acetate buffer containing 2.5% by volume DMSO. $[1] = 50 \mu\text{M}$, $[\text{meso-Tar}] = 3 \mu\text{M}$, $[\text{L-Tar}] + [\text{D-Tar}] = 27 \mu\text{M}$.

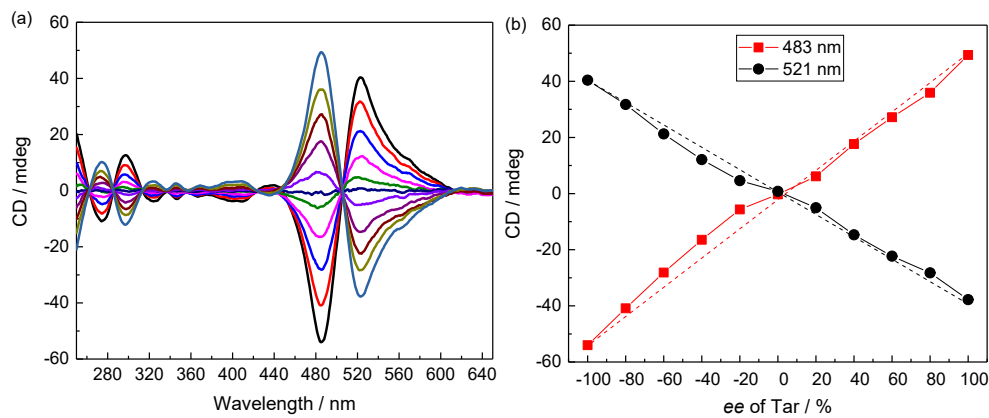


Figure S6. (a) CD spectra of **1** in the presence of Tar of different *ee* and (b) CD-*ee* dependence of **1**-Tar assembly in pH 5.0 acetate buffer containing 2.5% by volume DMSO. $[1] = 50 \mu\text{M}$, $[\text{meso-Tar}] = 6 \mu\text{M}$, $[\text{L-Tar}] + [\text{D-Tar}] = 24 \mu\text{M}$.

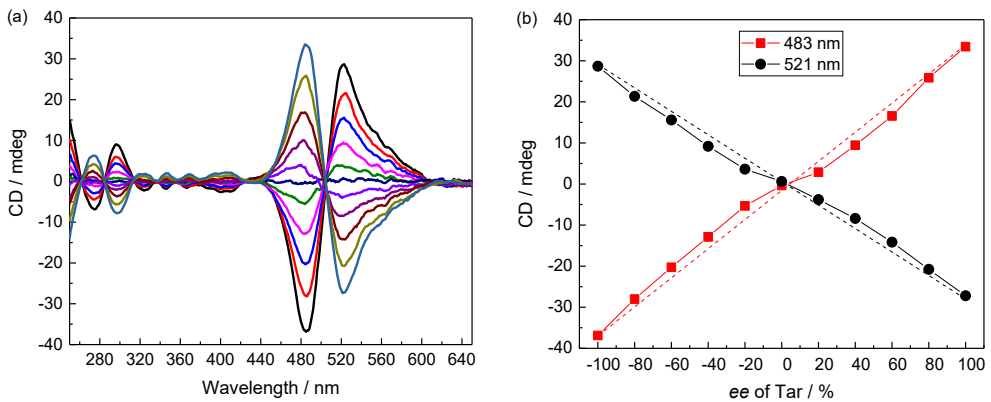


Figure S7. (a) CD spectra of **1** in the presence of Tar of different *ee* and (b) CD-*ee* dependence of **1**-Tar assembly in pH 5.0 acetate buffer containing 2.5% by volume DMSO. $[1] = 50 \mu\text{M}$. $[\text{meso-Tar}] = 9 \mu\text{M}$, $[\text{L-Tar}] + [\text{D-Tar}] = 21 \mu\text{M}$.

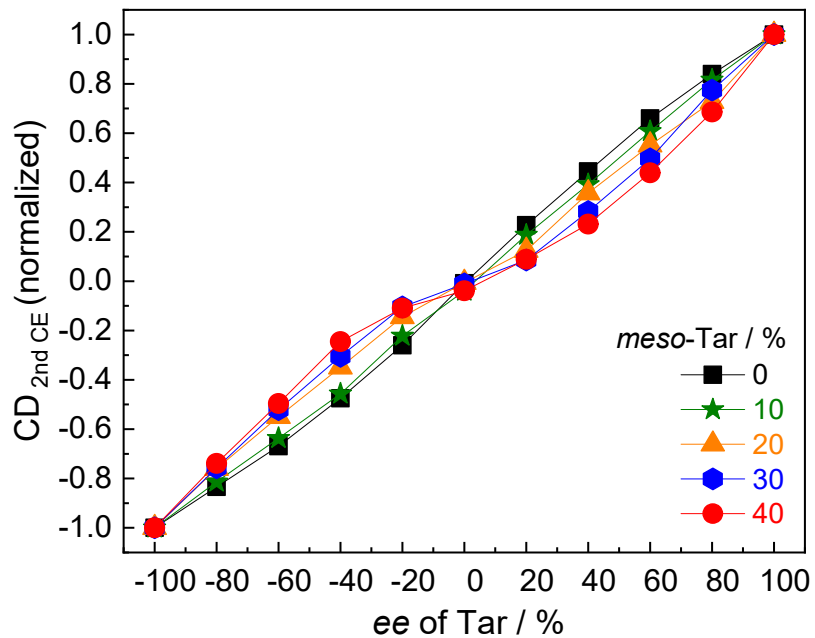


Figure S8. CD-*ee* dependence of **1**-Tar assembly versus *ee* of L- and D-tartaric acid in the mixture of meso-, L- and D-tartaric acid of increasing molar fraction of meso-Tar in pH 5.0 acetate buffer containing 2.5% by volume DMSO. Note that the curve turns from S- to anti-S-shaped when the molar fraction of meso-Tar is over 20%. $[1] = 50 \mu\text{M}$, $[\text{meso-Tar}] + ([\text{L-Tar}] + [\text{D-Tar}]) = 30 \mu\text{M}$.

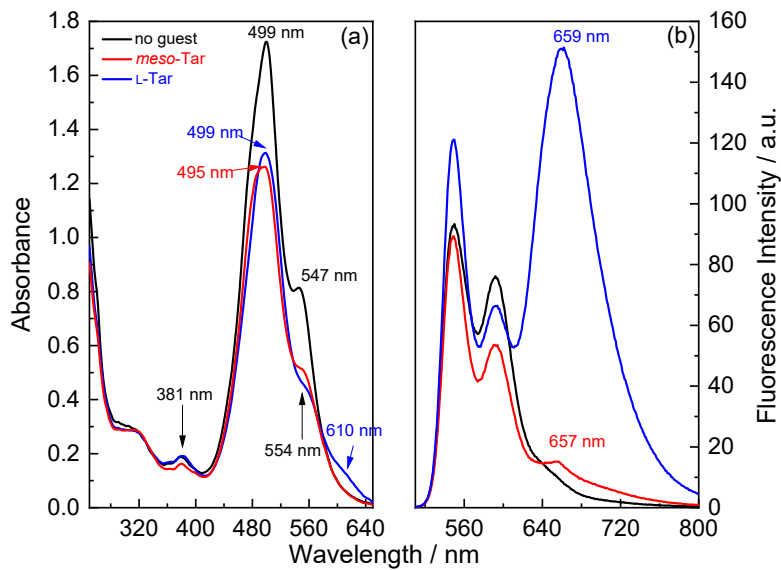


Figure S9. Absorption (a) and fluorescence (b) spectra of **1** in the absence (black lines) and in the presence of *meso*-Tar (red lines) and *L*-Tar (blue lines) in pH 5.0 acetate buffer containing 2.5% by volume DMSO. $[1] = 50 \mu\text{M}$, $[\text{Tar}] = 30 \mu\text{M}$.

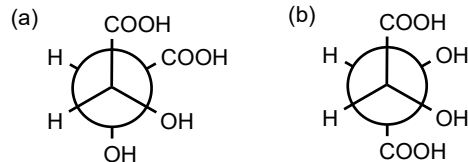


Figure S10. The most stable conformations of (a) *meso*-Tar and (b) *L*-Tar in aqueous solution.

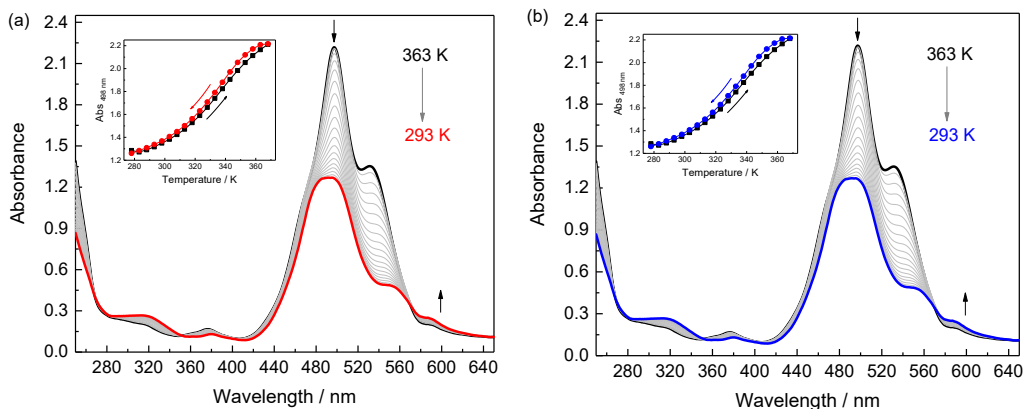


Figure S11. Temperature-dependent absorption spectra of (a) **1**-*meso*-Tar and (b) **1**-*L*-Tar assemblies during cooling from 363K to 293 K in pH 5.0 acetate buffer containing 2.5% by

volume DMSO. Insets are the corresponding cooling and heating curves of absorbance at 498 nm versus temperature. $[1] = 50 \mu\text{M}$, $[\text{Tar}] = 30 \mu\text{M}$.

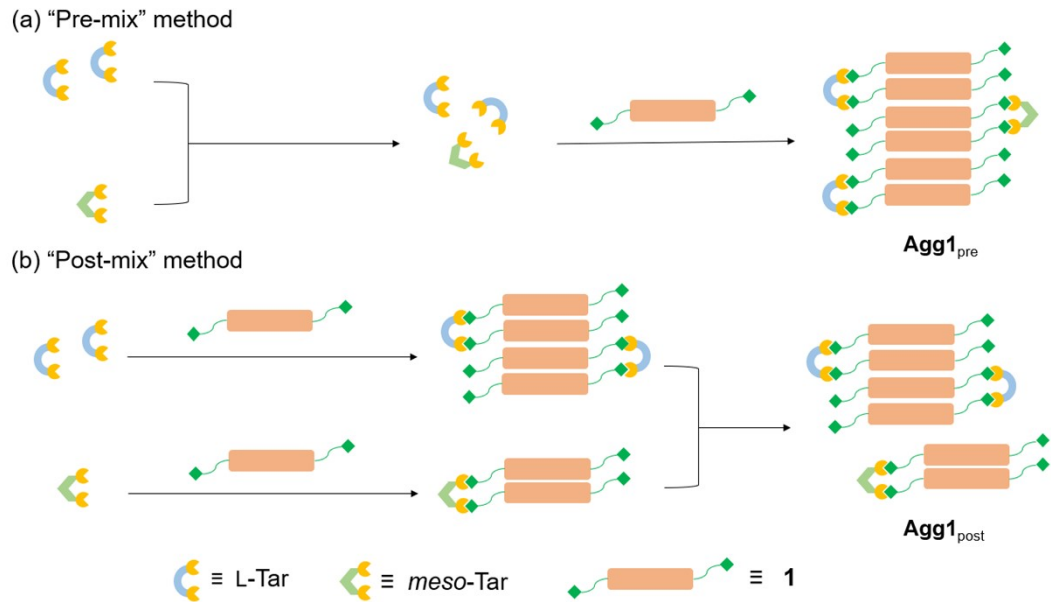


Figure S12. Schematic representation of pre-mix (a) and post-mix (b) methods.

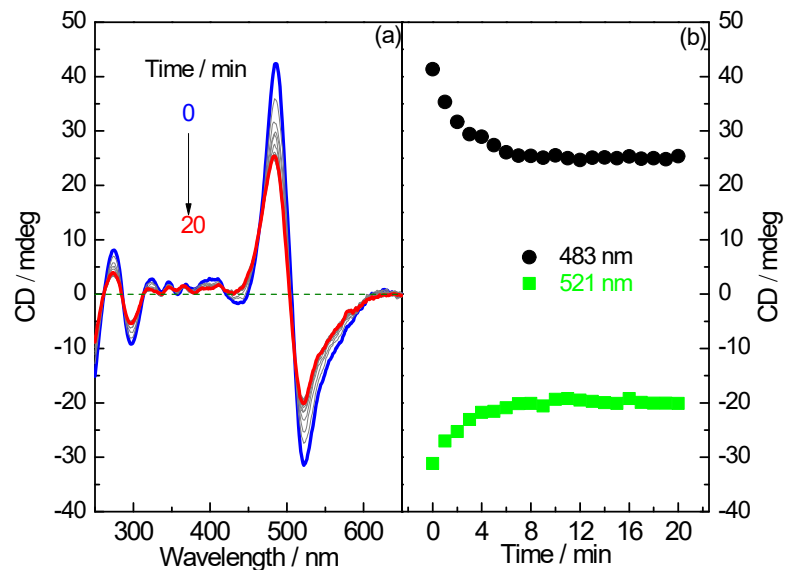


Figure S13 (a) Time-dependent CD spectra of a mixture of **1** (30 μM)/L-Tar (18 μM) assembly and **1** (20 μM)/meso-Tar (12 μM) assembly prepared by post-mix method in pH 5.0 acetate buffer containing 2.5% by volume DMSO. (b) Time profiles of CD signals at 483 and 521 nm.

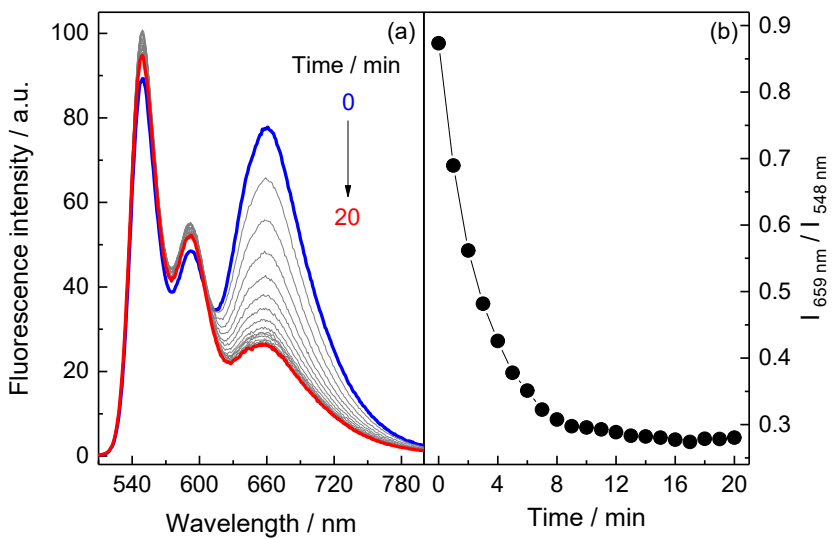


Figure S14. (a) Time-dependent fluorescence spectra of a mixture of **1** (30 μM)/L-Tar (18 μM) assembly and **1** (20 μM)/meso-Tar (12 μM) assembly prepared by post-mix method in pH 5.0 acetate buffer containing 2.5% by volume DMSO. (b) Time profile of the intensity ratio of excimer (659 nm) to monomer (548 nm) emission. $\lambda_{\text{ex}} = 499 \text{ nm}$, slit_{ex} = slit_{em} = 5 nm.

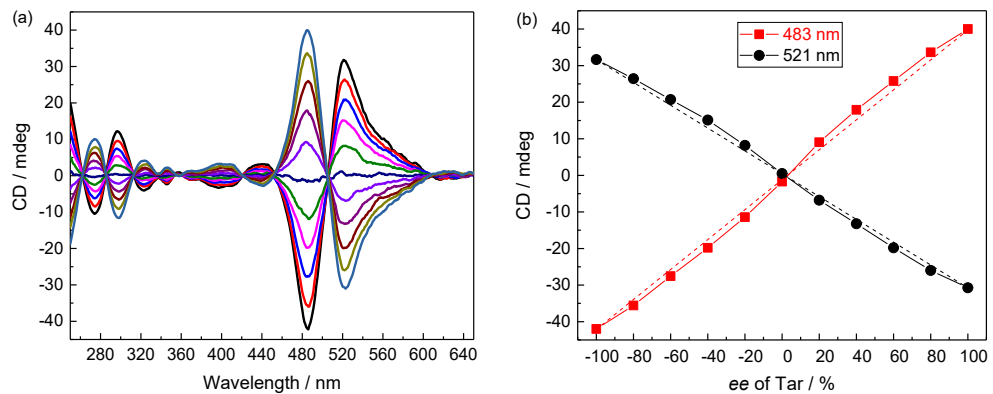


Figure S15. (a) CD spectra of **1** in the presence of Tar of varying ee and (b) CD-ee dependence of **1**-Tar assembly in pH 5.0 acetate buffer containing 2.5% by volume DMSO. $[1] = 50 \mu\text{M}$, $[\text{L-Tar}] + [\text{D-Tar}] = 18 \mu\text{M}$.